

Scattering off \mathcal{PT} -symmetric upside-down potentials

Carl M. Bender^{a,*} and Mariagiovanna Gianfreda^{a,b†}

^a *Department of Physics, Washington University, St. Louis, MO 63130, USA and*

^b *Institute of Industrial Science, University of Tokyo, Komaba, Meguro, Tokyo 153-8505, Japan*

The upside-down $-x^4$, $-x^6$, and $-x^8$ potentials with appropriate \mathcal{PT} -symmetric boundary conditions have real, positive, and discrete quantum-mechanical spectra. This paper proposes a straightforward macroscopic quantum-mechanical scattering experiment in which one can observe and measure these bound-state energies directly.

In 1998 the class of \mathcal{PT} -symmetric Hamiltonians

$$H = p^2 + x^2(ix)^\varepsilon \quad (1)$$

was introduced and it was shown numerically and perturbatively that even though these Hamiltonians are not Hermitian, their spectra are real, positive, and discrete if $\varepsilon > 0$ [1, 2]. A rigorous proof was given in Ref. [3]. This spectral positivity is particularly surprising for the case $\varepsilon = 2$ because on the real axis the $-x^4$ potential is upside-down and therefore appears to be unstable. Nevertheless, for this special value of ε there is an elementary transformation which establishes that the Hamiltonians $H = p^2 - x^4$ and $H = 2p^2 + 4x^4 - 2x$ are *isospectral*; that is, the eigenvalues of these two Hamiltonians are identical [4–6]. Since the potential of the latter Hamiltonian is conventionally right-side-up, its bound-state eigenvalues are indeed real, positive, and discrete. The numerical values of the first three bound-state energies are

$$E_0 = 1.477150, \quad E_1 = 6.003386, \quad E_2 = 11.802434. \quad (2)$$

One might think that it is physically impossible for an upside-down potential such as $-x^4$ to confine bound states because this potential is unbounded below. However, the \mathcal{PT} -symmetric eigenvalue problem for this potential must be formulated in the complex- x plane, and if we continue from real x to complex x , we lose the ordering principle; that is, if x_1 and x_2 are complex, we cannot say that $x_1 > x_2$ or $x_1 < x_2$. Thus, the concept of a potential $V(x)$ being unbounded below is not relevant when x is complex because the apparent instability of the $-x^4$ potential evaporates when x is complex [7].

The objective of this paper is to show that even though the eigenvalue problem for the $-x^4$ potential is formulated in the complex- x plane, it is actually possible to *observe and measure* the bound-state energies of the $-x^4$ potential with a conceptually simple scattering experiment. The underlying idea may be found in Ref. [8], where it is shown that the $-x^4$ potential becomes reflectionless if the energy of the incident wave is equal to one of the bound-state-energy eigenvalues. Furthermore, we will show that the bound-state energies of the upside-down \mathcal{PT} -symmetric $-x^6$ and $-x^8$ potentials can also be seen and measured by using scattering experiments.

To explain the reflectionless property of upside-down \mathcal{PT} -symmetric potentials, we note that the bound-state solutions to the time-independent Schrödinger equation for the $-x^4$ potential

$$-\phi''(x) - x^4\phi(x) = E\phi(x) \quad (3)$$

are required to vanish exponentially in an appropriate pair of Stokes wedges in the complex- x plane. To find the angular orientation of these Stokes wedges we construct the WKB approximation to the solutions to (3):

$$\phi_{\text{WKB}}(x) = C_\pm [Q(x)]^{-1/4} \exp\left[\pm i \int^x ds \sqrt{Q(s)}\right], \quad (4)$$

where $Q(x) = E + x^4$. Thus, for large $|x|$ the exponential component of the asymptotic behavior of $\phi(x)$ is

$$\phi(x) \sim e^{\pm ix^3/3} \quad (|x| \rightarrow \infty). \quad (5)$$

From (5) we see that there are six possible Stokes wedges in the complex- x plane, each having an opening angle of $\pi/3$, inside of which $\phi(x)$ can vanish exponentially. As explained in Ref. [9], we require that $\phi(x)$ vanish in a \mathcal{PT} -symmetric pair of Stokes wedges that are symmetric with respect to the imaginary- x axis. Substituting $x = re^{i\theta}$ in (5), we see that the angular range of the right Stokes wedge, which is located adjacent to and just below the positive-real- x axis, is $-\pi/3 < \theta < 0$, so we must choose the *minus* sign in (5):

$$\phi(x) \sim e^{-ix^3/3} \quad (|x| \rightarrow \infty, \quad -\pi/3 < \arg x < 0). \quad (6)$$

The angular range of the left Stokes wedge, which is a \mathcal{PT} reflection of the right Stokes wedge, is $-\pi < \theta < -2\pi/3$, so again we choose the minus sign in (5):

$$\phi(x) \sim e^{-ix^3/3} \quad (|x| \rightarrow \infty, \quad -\pi < \arg x < -2\pi/3). \quad (7)$$

Equations (6) and (7) indicate that if we rotate (anticlockwise in the right wedge and clockwise in the left wedge) to the upper edges of these wedges, which lie along the real axis, the eigenfunctions no longer decay exponentially and instead they represent purely oscillatory unidirectional waves [apart from an algebraic factor of $1/|x|$ coming from the WKB approximation in (4)].

Similarly, for the upside-down $-x^6$ potential, which is obtained by setting $\varepsilon = 2$ in the \mathcal{PT} -symmetric $x^4(ix)^\varepsilon$ potential, there are two Stokes wedges of opening angle $\pi/4$ lying adjacent to and just below the real- x axis. On the real- x axis the bound-state eigenfunctions, which decay approximately like $\exp(-|x|^4)$ in these Stokes wedges, represent purely oscillatory unidirectional waves

$$\phi(x) \sim e^{-ix^4/4} \quad (x \rightarrow \pm\infty) \quad (8)$$

(apart from an algebraic factor of $|x|^{-3/2}$). The first three bound-state energies of the $-x^6$ potential are

$$E_0 = 1.354862, \quad E_1 = 5.262586, \quad E_2 = 11.234957. \quad (9)$$

Likewise, for the upside-down $-x^8$ potential, which is obtained by setting $\varepsilon = 2$ in the \mathcal{PT} -symmetric $x^6(ix)^\varepsilon$ potential, there are two Stokes wedges of opening angle $\pi/5$ lying adjacent to and just below the real- x axis. On the real- x axis the bound-state eigenfunctions, which decay approximately like $\exp(-|x|^5)$ in these Stokes wedges, represent purely oscillatory unidirectional waves

$$\phi(x) \sim e^{-ix^5/5} \quad (x \rightarrow \pm\infty) \quad (10)$$

(apart from an algebraic factor of $|x|^{-2}$). The first three bound-state energies of the $-x^8$ potential are

$$E_0 = 1.359859, \quad E_1 = 5.320461, \quad E_2 = 11.559893. \quad (11)$$

To summarize, *at the bound-state energy eigenvalues of the \mathcal{PT} -symmetric $-x^4$ (and $-x^6$ and $-x^8$) potentials the eigenfunctions exhibit asymptotically unidirectional wave propagation.* This implies that, at least in principle, we can identify the bound-state energies by performing a scattering experiment and looking for unidirectional incoming and outgoing waves, that is, reflectionless scattering. However, performing an actual scattering experiment is not trivial because these upside-down potentials increase in strength as $|x|$ increases and they become infinite at $|x| = \infty$. Thus, in the laboratory it is necessary to confine the potential to a finite-size box and thus we must study the *cut-off* version of the potential.

Let us consider a one-dimensional scattering experiment in which the cut-off potential $V(x)$ vanishes outside a box of size $2L$:

$$V(x) = \begin{cases} 0 & (|x| > L), \\ -x^4 & (|x| \leq L). \end{cases} \quad (12)$$

The time-dependent Schrödinger equation that describes a scattering process in the potential $V(x)$ is

$$i\psi_t(x, t) = -\psi_{xx}(x, t) + V(x)\psi(x, t). \quad (13)$$

In a time-independent scattering experiment we take the incident wave to be a monochromatic plane wave of energy E so that the time dependence of $\psi(x, t)$ is simply

$$\psi(x, t) = e^{-iEt}\phi(x)$$

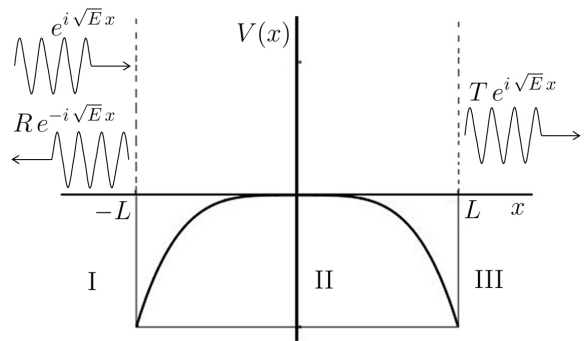


FIG. 1: Time-independent scattering experiment showing an upside-down potential in a box of size $2L$ and the incident and reflected plane waves of energy E in (15) and the transmitted plane wave of energy E in (16).

and (13) reduces to a time-independent Schrödinger equation of the form in (3):

$$-\phi''(x) + V(x)\phi(x) = E\phi(x). \quad (14)$$

Thus, a plane wave of the form $\phi(x) = e^{iax}$ is a *right-going* wave if $a > 0$ and a *left-going* wave if $a < 0$.

There are three regions for $V(x)$ in (12) depending on whether $x < -L$ (Region I), $-L \leq x \leq L$ (Region II), and $x > L$ (Region III) (see Fig. 1). In Region I we assume that we have a right-going *incident plane wave* of unit amplitude and energy E plus a left-going *reflected plane wave* of amplitude R and energy E :

$$\phi_I(x) = e^{ix\sqrt{E}} + R e^{-ix\sqrt{E}}. \quad (15)$$

In Region III we assume that we have a right-going *transmitted plane wave* of amplitude T and energy E :

$$\phi_{III}(x) = T e^{ix\sqrt{E}}. \quad (16)$$

We then define the scaled wave function $y(x)$,

$$y(x) \equiv \phi(x)e^{-iL\sqrt{E}}/T, \quad (17)$$

and we impose the following outgoing-wave boundary conditions at $x = L$:

$$y_{III}(L) = 1, \quad y'_{III}(L) = i\sqrt{E}. \quad (18)$$

Using these boundary conditions, we perform a numerical integration of the time-independent Schrödinger equation (14) from $x = L$ down to $x = -L$ and compare the numerical results with the boundary conditions at $x = -L$, which are

$$\begin{aligned} y_I(-L) &= e^{-2iL\sqrt{E}}/T + R/T, \\ y'_I(-L) &= i\sqrt{E}e^{-2iL\sqrt{E}}/T - iR\sqrt{E}/T. \end{aligned} \quad (19)$$

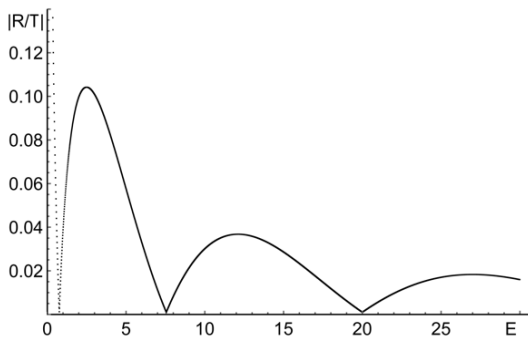


FIG. 2: Plot of $|R/T|$ in (20) as a function of E for $L = 1$. The vanishing of this ratio indicates that there is resonant (reflectionless) scattering. Note that $|R/T|$ vanishes at $E = 0.76, 7.55,$ and 19.99 . However, comparing this figure with Figs. 3 and 4, we see that the energies at which resonant (reflectionless) scattering occurs depend on L . Furthermore, these zeros do not agree with the eigenvalues in (2).

This gives an explicit form for the ratio $|R/T|$:

$$|R/T| = \frac{1}{2} |y_{\text{I}}(-L) + iy'_{\text{I}}(-L)/\sqrt{E}|. \quad (20)$$

In Figs. 2–4 we plot the computed numerical ratio $|R/T|$ in (20) for $L = 1, 2,$ and 5 . Observe that the zeros of $|R/T|$ depend on the value of L . Furthermore, these zeros are clearly not related to the eigenvalues in (2). Therefore, if in this experiment the incident, reflected, and transmitted plane waves have energy E , we cannot measure the \mathcal{PT} -symmetric bound-state energies. Evidently, this way of performing the scattering experiment is not successful because the zeros of $|R/T|$ shown in Figs. 2–4 are merely the conventional resonant scattering energies of the potential $V(x)$ at which the potential becomes reflectionless. These resonant energies *depend on the size $2L$ of the box*.

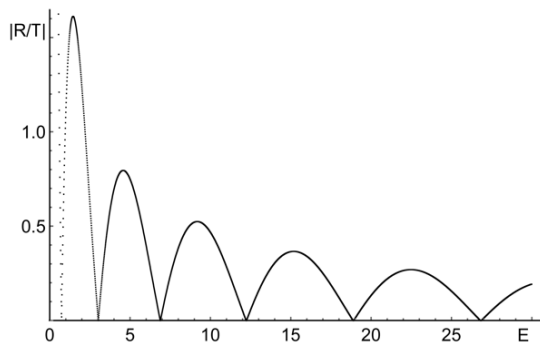


FIG. 3: Plot of the ratio $|R/T|$ in (20) as a function of E for $L = 2$. The zeros at which resonant scattering occurs are now located at $E = 0.74, 3.02, 6.88, 12.23,$ and 26.83 and they have moved from their positions in Fig. 2. This shows that the resonant scattering energies depend on L .

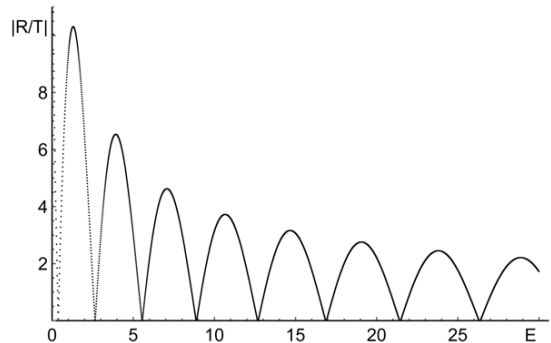


FIG. 4: Plot of $|R/T|$ in (20) as a function of E for $L = 5$. The zeros are now located at $E = 0.38, 2.75, 5.55, 8.89, 12.68, 16.88, 21.44,$ and 26.34 .

There *is* a way to perform a time-independent scattering experiment in which we can observe the energy levels in (2). Using plane waves only, we take the energies of the incident, reflected, and transmitted waves in Regions I and III to *depend on L* . To understand why this works, let us examine more carefully the WKB approximation to the solution to the time-independent Schrödinger equation (3). Because the WKB approximation to $\phi(x)$ has the form in (4), we choose the following L -dependent boundary conditions on the positive- x axis at $x = L$:

$$\phi_{\text{III}}(L) = 1, \quad \phi'_{\text{III}}(L) = i\sqrt{Q(L)} - \frac{1}{4}Q'(L)/Q(L). \quad (21)$$

To obtain these simple boundary conditions we have set $C_- = 0$ in (4) (because in Region III there are only right-going waves) and we have chosen C_+ so that

$$\phi_{\text{WKB}}(x) = \left[\frac{Q(L)}{Q(x)} \right]^{1/4} \exp \left[i \int_L^x ds \sqrt{Q(s)} \right].$$

Of course, to justify the using a WKB approximation we must assume that L is large and that x is near L .

Then, on the negative- x axis we take a WKB approximation of the form

$$\phi_{\text{WKB}}(x) = \left[\frac{Q(L)}{Q(x)} \right]^{1/4} \left(D_- \exp \left[-i \int_{-L}^x ds \sqrt{Q(s)} \right] + D_+ \exp \left[i \int_{-L}^x ds \sqrt{Q(s)} \right] \right),$$

where we assume that x is near $-L$. (Note here that D_+ is the coefficient of the right-going incident wave and D_- is the coefficient of the left-going reflected wave.) From this formula we calculate

$$\phi_{\text{I}}(-L) = D_- + D_+$$

and

$$\begin{aligned} \phi'_{\text{I}}(-L) &= D_- \left[-i\sqrt{Q(L)} - \frac{1}{4}Q'(L)/Q(L) \right] \\ &\quad + D_+ \left[i\sqrt{Q(L)} - \frac{1}{4}Q'(L)/Q(L) \right]. \end{aligned}$$

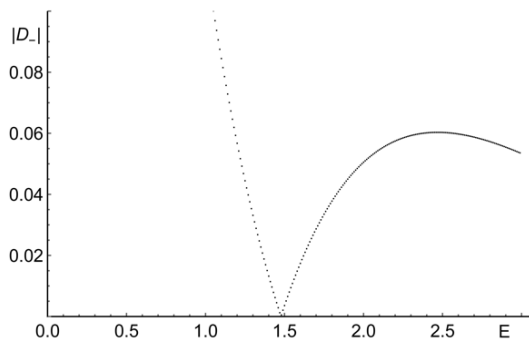


FIG. 5: Plot of $|D_-|$ in (22) as a function of E for $L = 5$. There is a zero at $E = 1.475$, which is in very good agreement with the exact value of the ground-state energy 1.477 in (2).

Thus,

$$|D_-| = \frac{1}{2} \left| \left[i - \frac{Q'(L)}{4Q^{3/2}(L)} \right] \phi(-L) - \frac{\phi'(-L)}{\sqrt{Q(L)}} \right|. \quad (22)$$

We now integrate the Schrödinger equation (3) from L to $-L$ using the boundary conditions (21) and calculate $\phi_I(-L)$ and $\phi'_I(-L)$ numerically. Then from (22) we calculate the coefficient D_- of the reflected wave in Region I. In Figs. 5–7 we plot $|D_-|$. Note that $|D_-|$ vanishes at the bound-state energies of the $-x^4$ potential in (2).

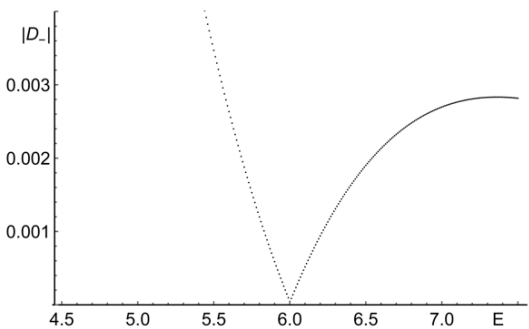


FIG. 6: Plot of $|D_-|$ in (22) as a function of E for $L = 5$. The zero lies at $E = 6.005$, which is an accurate approximation to the exact value of the first energy level 6.003 in (2).

Our results for the $-x^4$ potential immediately generalize to other upside-down potentials. For a $-x^6$ potential we take $Q(x) = E + x^6$. The analogs of Figs. 5–7 are Figs. 8–10. For a $-x^8$ potential we take $Q(x) = E + x^8$ and the analogs of Figs. 5–7 are Figs. 11–13.

To conclude, we emphasize that the spectrum of an upside-down \mathcal{PT} -symmetric potential is real, positive, and discrete. This remarkable and rigorous mathematical result reflects the nature of boundary-value problems in the complex domain. However, in this paper we have shown that it is possible to observe these eigenvalues in the laboratory by using a simple macroscopic

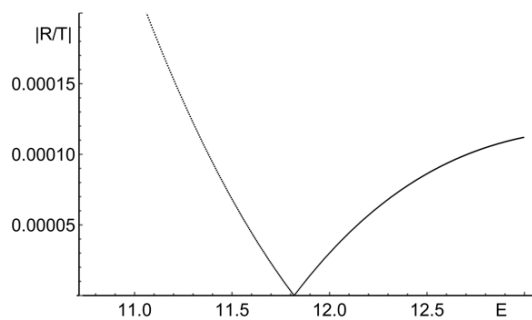


FIG. 7: Plot of $|D_-|$ in (22) as a function of E for $L = 7$. The zero at 11.820 is an accurate approximation to the exact value of the second energy level 11.802 in (2). If we take $L = 5$, the zero is at $E = 11.700$, which is not quite as accurate.

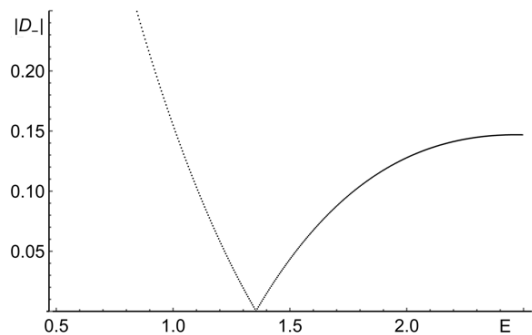


FIG. 8: Plot of $|D_-|$ for the $-x^6$ potential for $L = 5$. There is a zero at 1.355, which agrees with $E_0 = 1.355$ in (9).

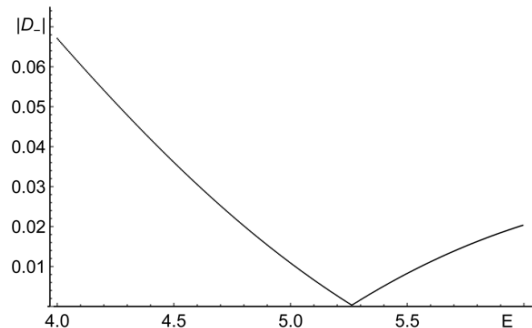


FIG. 9: Plot of $|D_-|$ for the potential $-x^6$ for $L = 5$. The zero at 5.270 agrees with the exact value of $E_1 = 5.263$ in (9).

time-independent quantum-mechanical scattering experiment. (To produce an upside-down $-x^4$ potential in a box one might superpose a cosine potential associated with the Josephson effect with a parabolic potential.) Many experimental studies of classical \mathcal{PT} -symmetric systems have been done [11–19] but these experiments have focused on the classical \mathcal{PT} phase transition. The experiment proposed in this paper would be the first ex-

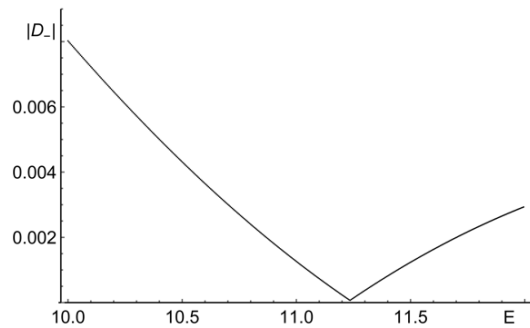


FIG. 10: Plot of $|D_-|$ for the potential $-x^6$ for $L = 5$. The zero at 11.240 agrees with the exact value $E_2 = 11.235$ in (9).

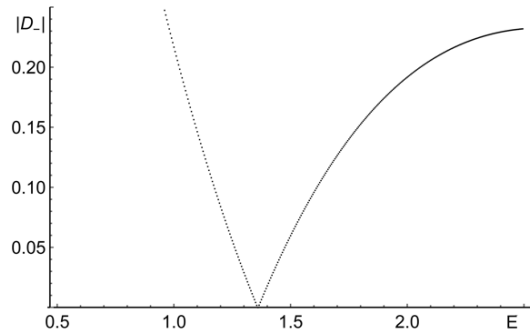


FIG. 11: Plot of $|D_-|$ for the potential $-x^8$ for $L = 5$. The zero at 1.360 compares well with $E_0 = 1.359$ in (11).

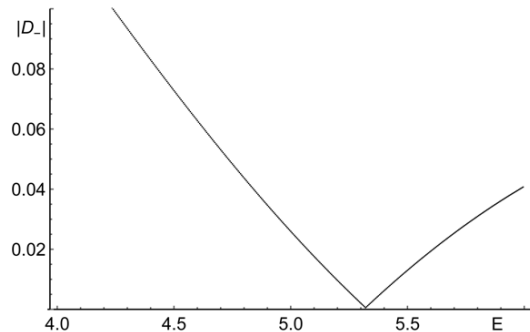


FIG. 12: Plot of $|D_-|$ for the potential $-x^8$ for $L = 5$. The zero at 5.320 compares well with $E_1 = 5.320$ in (11).

perimental examination of the bound-state spectrum of a quantum-mechanical \mathcal{PT} -symmetric system.

We thank D. Hook for precise numerical calculations of bound-state energies and K. Murch for discussions about experimental possibilities.

* Electronic address: cmb@wustl.edu

† Electronic address: Maria.Gianfreda@le.infn.it

- [1] C. M. Bender and S. Boettcher, Phys. Rev. Lett. **80**, 5243 (1998).
- [2] C. M. Bender, S. Boettcher, and P. N. Meisinger J. Math. Phys. **40**, 2201 (1999).
- [3] P. E. Dorey, C. Dunning, and R. Tateo, J. Phys. A: Math. Theor. **40**, R205 (2007).
- [4] V. Buslaev and V. Grecchi, J. Phys. A: Math. Gen. **26**, 5541 (1993).
- [5] H. F. Jones and J. Mateo, Phys. Rev. D **73**, 085002 (2006).
- [6] C. M. Bender, D. C. Brody, J.-H. Chen, H. F. Jones, K. A. Milton, and M. C. Ogilvie, Phys. Rev. D **74**, 025016 (2006).
- [7] C. M. Bender, D. W. Hook, N. E. Mavromatos, and S. Sarkar, arXiv: hep-th/1506.01970.
- [8] Z. Ahmed, C. M. Bender, and M. V. Berry, J. Phys. A: Math. Gen. **38**, L627 (2005).
- [9] C. M. Bender, Rept. Prog. Phys. **70**, 947-1018 (2007).
- [10] J. Rubinstein, P. Sternberg, and Q. Ma, Phys. Rev. Lett. **99**, 167003 (2007).
- [11] A. Guo, G. J. Salamo, D. Duchesne, R. Morandotti, M. Volatier-Ravat, V. Aimez, G. A. Siviloglou, and D. N. Christodoulides, Phys. Rev. Lett. **103**, 093902 (2009).
- [12] C. E. Rüter, K. G. Makris, R. El-Ganainy, D. N. Christodoulides, M. Segev, and D. Kip, Nat. Phys. **6**, 192-195 (2010).
- [13] K. F. Zhao, M. Schaden, and Z. Wu, Phys. Rev. A **81**, 042903 (2010).
- [14] Z. Lin, H. Ramezani, T. Eichelkraut, T. Kottos, H. Cao, and D. N. Christodoulides, Phys. Rev. Lett. **106**, 213901 (2011).
- [15] L. Feng, M. Ayache, J. Huang, Y.-L. Xu, M. H. Lu, Y. F. Chen, Y. Fainman, and A. Scherer, Science **333**, 729 (2011).
- [16] J. Schindler, A. Li, M. C. Zheng, F. M. Ellis, and T. Kottos, Phys. Rev. A **84**, 040101(R) (2011).
- [17] S. Bittner, B. Dietz, U. Günther, H. L. Harney, M. Miski-Oglu, A. Richter, and F. Schäfer, Phys. Rev. Lett. **108**, 024101 (2012).
- [18] N. Chtchelkatchev, A. Golubov, T. Baturina, and V. Vinokur, Phys. Rev. Lett. **109**, 150405 (2012).
- [19] B. Peng, S. K. Ozdemir, F. Lei, F. Monifi, M. Gianfreda, G. L. Long, S. Fan, F. Nori, C. M. Bender, L. Yang, Nat. Phys. **10**, 394 (2014).

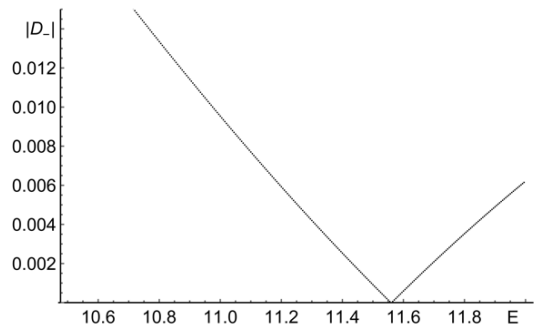


FIG. 13: Plot of $|D_-|$ for the potential $-x^8$ for $L = 5$. The zero at 11.560 compares well with $E_2 = 11.560$ in (11).